# Supporting Information

## Achieving Desirable Charge Transport by Porous Frame Engineering for Superior 3D Printed Rechargeable Ni-Zn Alkaline Batteries

# 1. Experimental Section

## *1.1 Materials*

All reagents were of analytical grade. $Ni(NO_3)_2 \cdot 6H_2O$ (>98.0%), $Co(NO_3)_2 \cdot 6H_2O$ (>98.5%), N-methyl-2-pyrrolidone (NMP, 99.5%), super P, polyvinylidene difluoride (PVDF), KOH (>85.0%), and hexamethylene tetramine ($C_6H_{12}N_4$, >99.0%), ethanol (>99.7%) were directly purchased from Sinopharm Chemical Reagent Co., Ltd. ZnO (>99.99%) was purchased from Shanghai Aladdin Biochemical Technology Co., Ltd.

## *1.2 Preparation of NiCo-LDH powders*

NiCo-LDH powders were synthesized using a typical method.[1] Firstly, 0.582 g $Co(NO_3)_2 \cdot 6H_2O$, 0.58g $Ni(NO_3)_2 \cdot 6H_2O$, and 1.12 g $C_6H_{12}N_4$ was added in 40 mL deionized (DI) water and stirred for 40 min. Afterwards, the obtained solution was transferred into a Teflon-lined stainless-steel autoclave and kept at 100°C for 10 h. After cooling to the room temperature, the products were centrifuged at 11,000 rpm for 5 min and washed for several times with DI water and ethanol. Finally, the drying procedure at 70°C for 12 h was conducted to obtain NiCo-LDH powders.

## *1.3 3D printing-based fabrication of NZAB electrodes*

In prior to the DIW-based 3D printing of NZAB electrodes, acid-etched nickel foam (A-NF) frame and NiCo-LDH/super P composite inks were fabricated, respectively. In a typical fabrication of A-NF, interdigital nickel foams (NFs) were immersed in 3 M HCl solution and then subjected to sonication for 30 min. Afterwards, the obtained A-

NFs were washed with DI water and subjected to sonication for 5 min.

Preparation of NiCo-LDH/super P inks: Firstly, 350 mg NiCo-LDH powder and 100 mg super P were added into a mortar, mixed with ethanol, and then kept at 70℃ for 12 h. 50 mg PVDF binder was then added into the fully dried mixture, and was further mixed evenly and grounded. Afterwards, 2100 μL NMP solvent was added into the above mixture to form printable NiCo-LDH/super P inks using a high-speed mixer.

As interdigital A-NF current collector frames were fixed onto target quartz glass substrates, the prepared inks were loaded into the 5 ml syringe with a nozzle of inner diameter of ~330 μm and printed into 3D current collector frames (with a mass loading of ~6.25 mg $cm^{-2}$ for cathode solids) using the 3-axis extrusion-based 3D printer. The initial distance between A-NF and nozzle was adjusted to ~0.2 mm, and the movement speed of syringe nozzle was set at 3 mm $s^{-1}$ under a pressure of 20 Kpa. Zn anode was further electrodeposited onto the other side of interdigital A-NFs using a two-electrode system, where the zinc plate acted as the counter electrode under the current of 5 mA in 2 M $ZnSO_4$ solution with different electrodeposited time. Finally, as-3D-printed electrodes were obtained after the freeze-dry, and ZnO-saturated 2 M KOH solution was used as electrolyte for resultant NZAB devices. Notably, the cell cases were 3D printed using the FDM 3D printer (Ultimaker S3), and the electrolyte was injected into sealed NZAB cell cases using a syringe.

### *1.4 Structural characterization and electrochemical measurements*

XRD patterns were collected on an X-ray diffractometer (Bruker D8 Discover) with Cu

Kα radiation (λ = 1.5418 Å). The morphologies of all materials and devices were characterized by the field-emission scanning electron microscope (Gemini SEM 300) equipped with EDS. CV and EIS measurements were conducted in a two-electrode system using an electrochemical workstation (CHI 760E). Land battery testing system was used for the galvanostatic charge-discharge (GCD) and rate capability test. The above electrochemical tests were conducted by sealing NZABs in 3D printed cases.

### *1.5 Calculation of device electrochemical performance*

Based on the measurement results, the device capacities of the NZABs were calculated using the following equation (1):

$$C = \frac{I}{S} \times t \tag{1}$$

where $C$ represented device areal capacities of NZABs, $I$ was the discharge current value, $S$ was total area of devices including the both interdigital macroelectrode area and interspace area, $t$ denoted the discharge time of NZABs.

The device areal energy densities of NZABs were calculated using the following equation (2):

$$E = I\frac{\int U(t)dt}{S} \tag{2}$$

where $E$ was the energy density of NZABs, $U(t)$ was voltage as a function of discharge time.

The device areal power densities ($P$) of NZABs were calculated using the following equation (3):

$$P = \frac{E}{t} \tag{3}$$

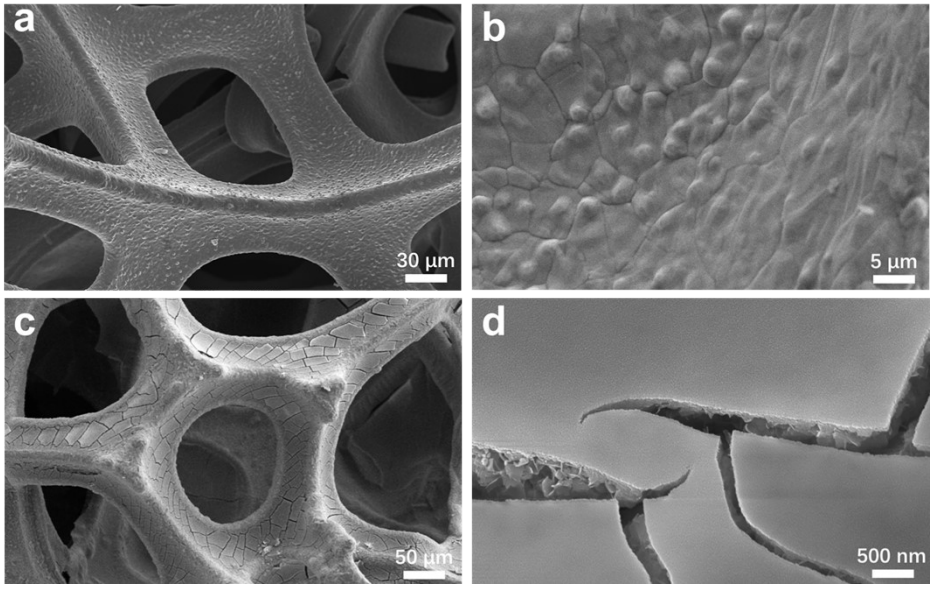


**Figure S1**. SEM images of NFs (a, b) and A-NFs (c, d).

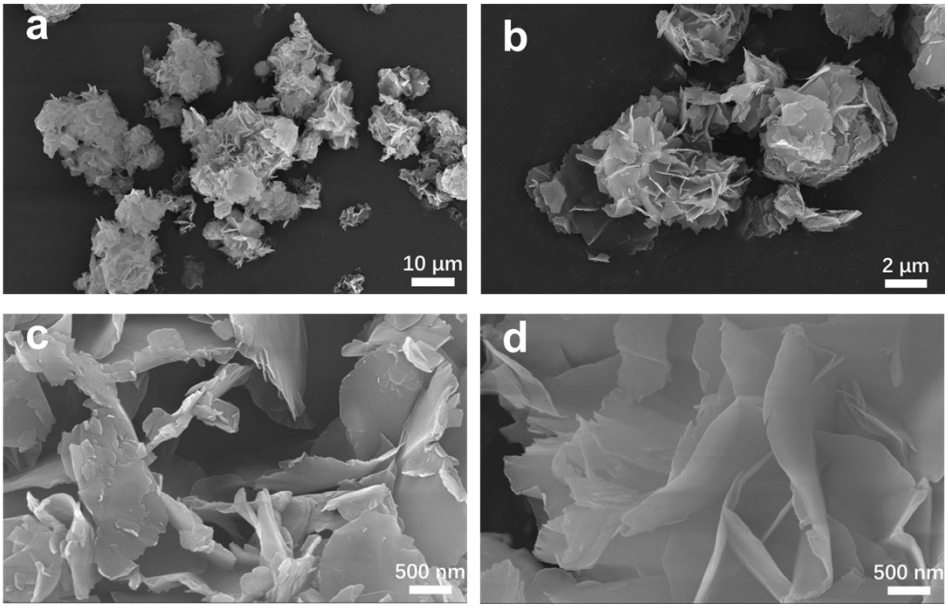


**Figure S2.** (a-d) SEM images of the NiCo-LDH powder.

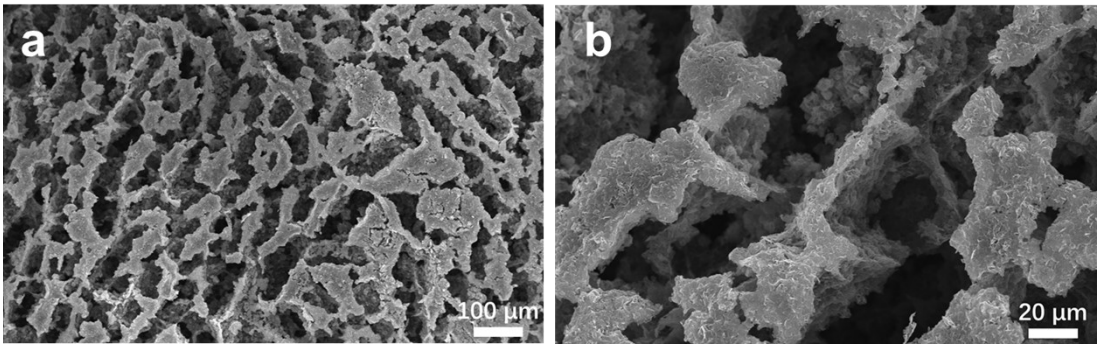


**Figure S3.** SEM images of Ni-based cathodes.

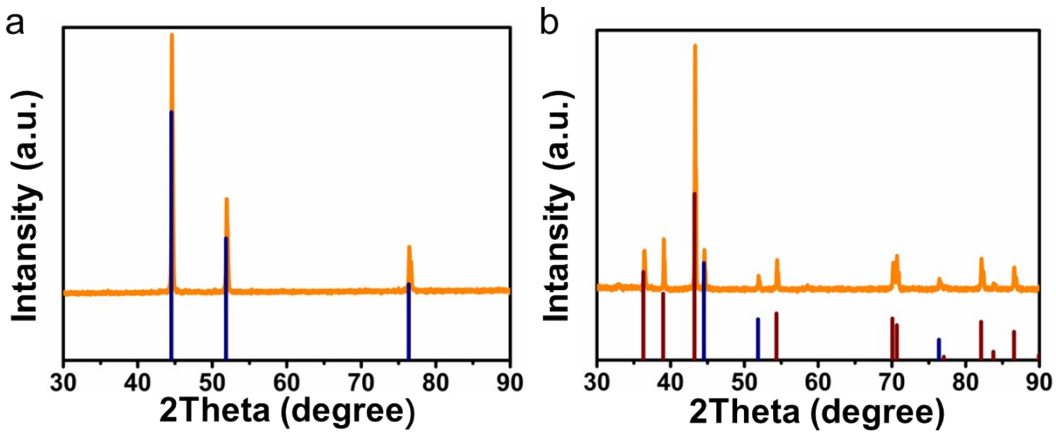


**Figure S4.** XRD patterns of NF frames (a) and Zn anodes (b).

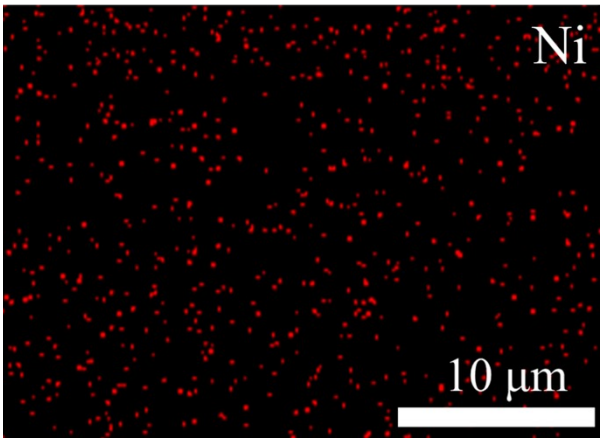


**Figure S5.** EDS mapping image of Zn anodes for the Ni element.

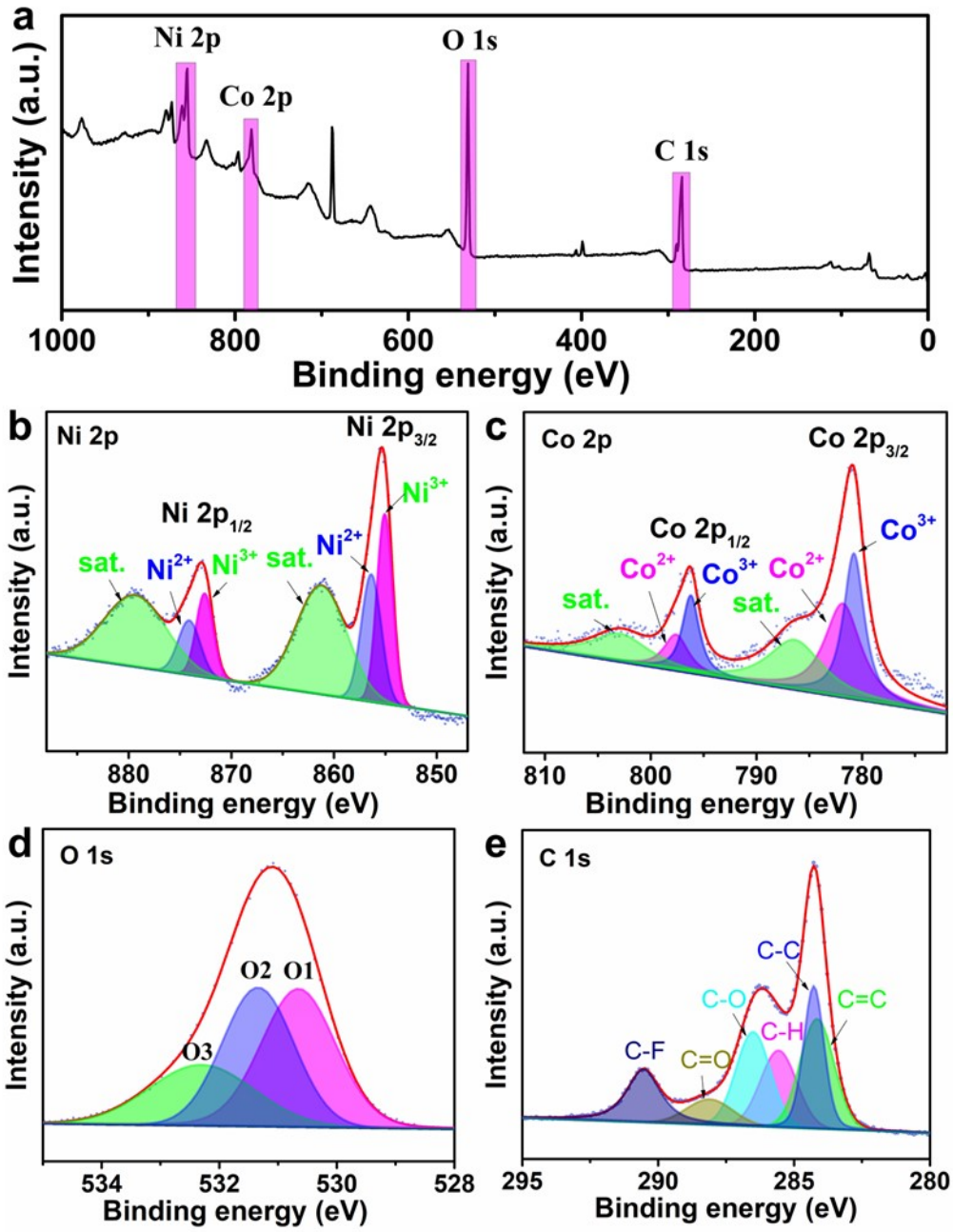


**Figure S6.** (a-e) XPS patterns of Ni-based cathode: the survey XPS spectra (a), Ni 2p (b), Co 2p (c), O 1s (d), and C 1s (e).

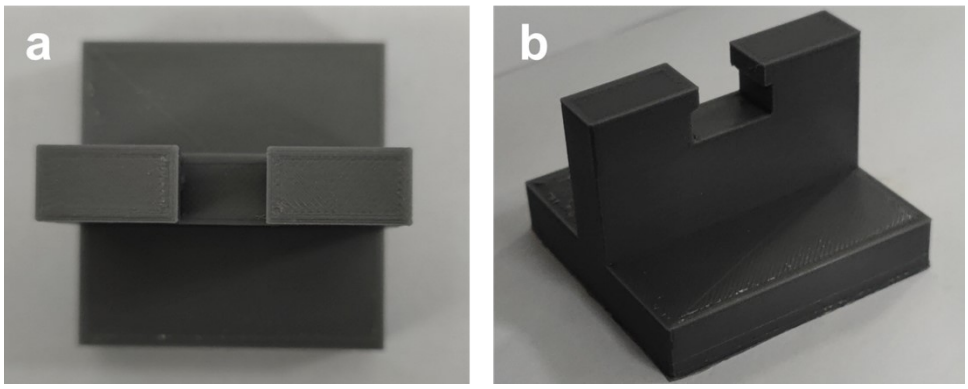


**Figure S7.** (a,b) Photographs of the holder for single-wired electrode characterization platform.

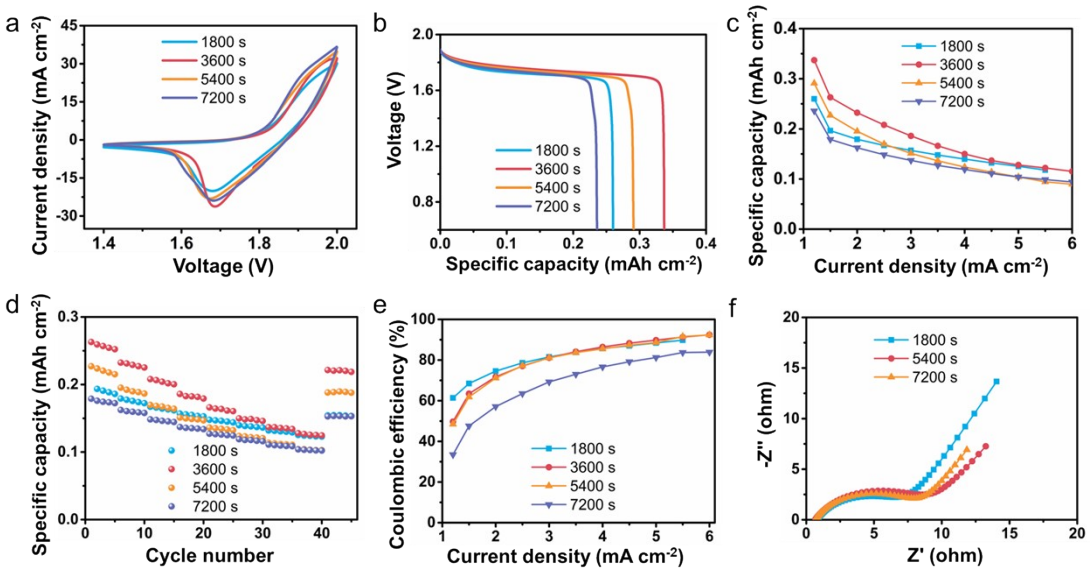


**Figure S8.** (a-f) Comparison of E3DP-NZABs with anodes electrodeposited at different time. (a) CV curves at a scan rate of 10 mV $s^{-1}$. (b) Galvanostatic discharge curves at a current density of 1.2 mA $cm^{-2}$. (c) Device capacity profiles. (d) Rate performance. (e) Coulombic efficiency profiles. (f) EIS curves.

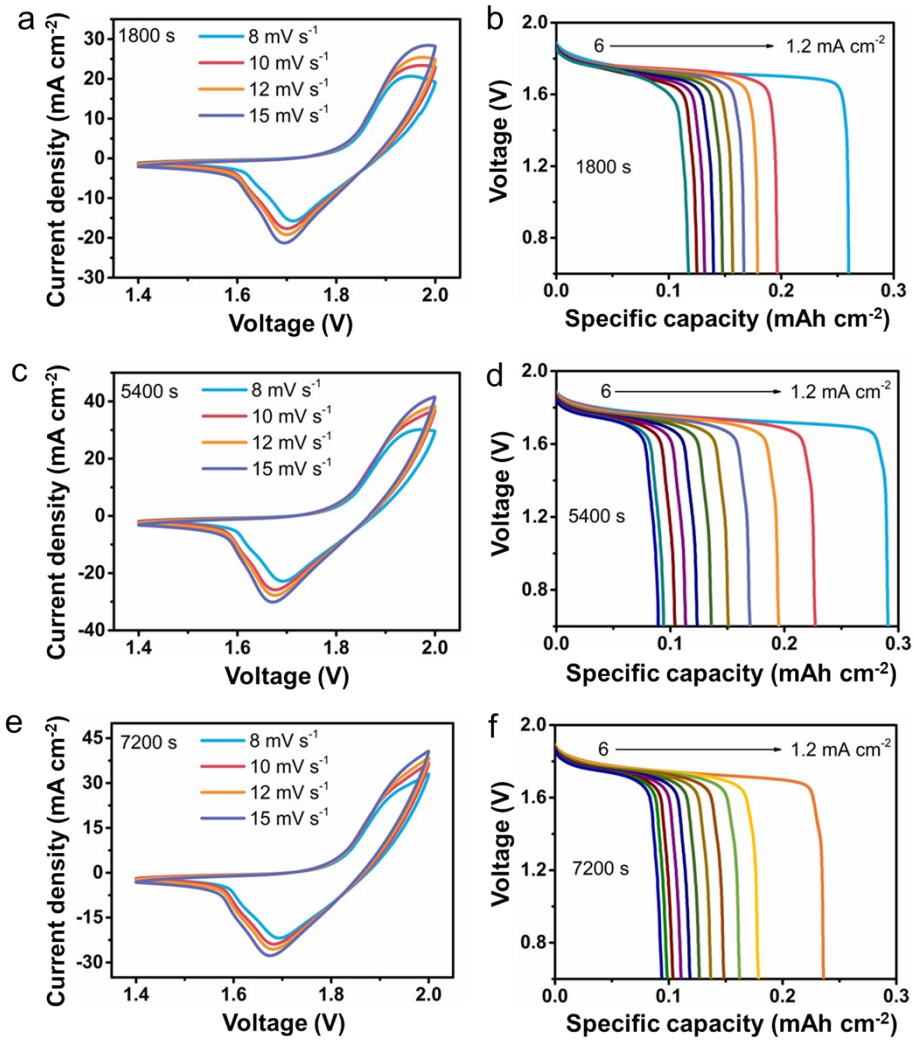


**Figure S9.** (a,b) CV (a) and galvanostatic discharge curves (b) of E3DP-NZABs with 1800 s electrodeposited anodes. (c,d) CV (c) and galvanostatic discharge curves (d) of E3DP-NZABs with 5400 s electrodeposited anodes. (e,f) CV (c) and galvanostatic discharge curves (d) of E3DP-NZABs with 7200 s electrodeposited anodes.

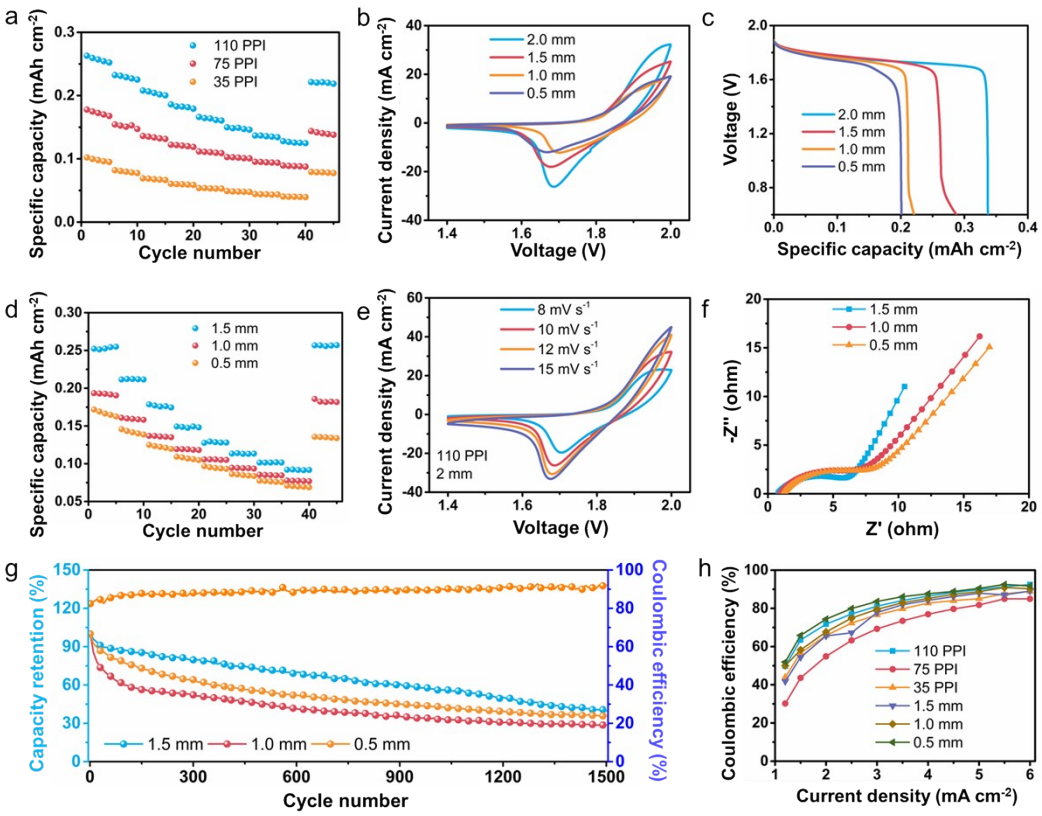


**Figure S10.** (a) Rate performance of E3DP-NZABs with different pore-sized 3D structure frames. (b-f) CV curves (b), galvanostatic discharge curves (c), rate performance (d), CV curves of E3DP-NZABs with 110 PPI (pore size) and 2 mm (thickness) (e), EIS curves (f), long-term cycling performance of E3DP-NZABs with different thickness of 3D structure frames (g). (h) Coulombic efficiency of E3DP-NZABs with different 3D structure frames.

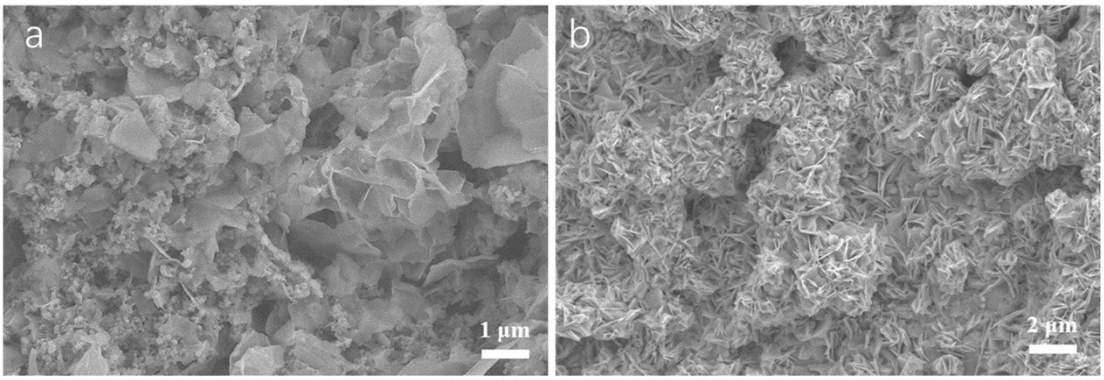


**Figure S11.** (a,b) SEM images of Ni-based cathodes (a) and Zn-based anodes (b) after cycling.

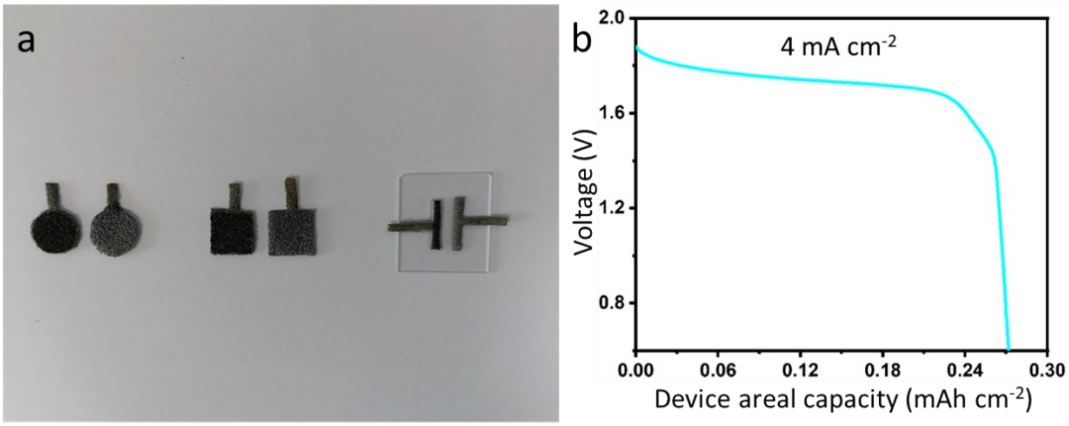


**Figure S12**. (a) Photograph of E3DP-NZAB electrodes in various geometries. (b) Discharge curve of E3DP-NZABs in a rectangular geometry.

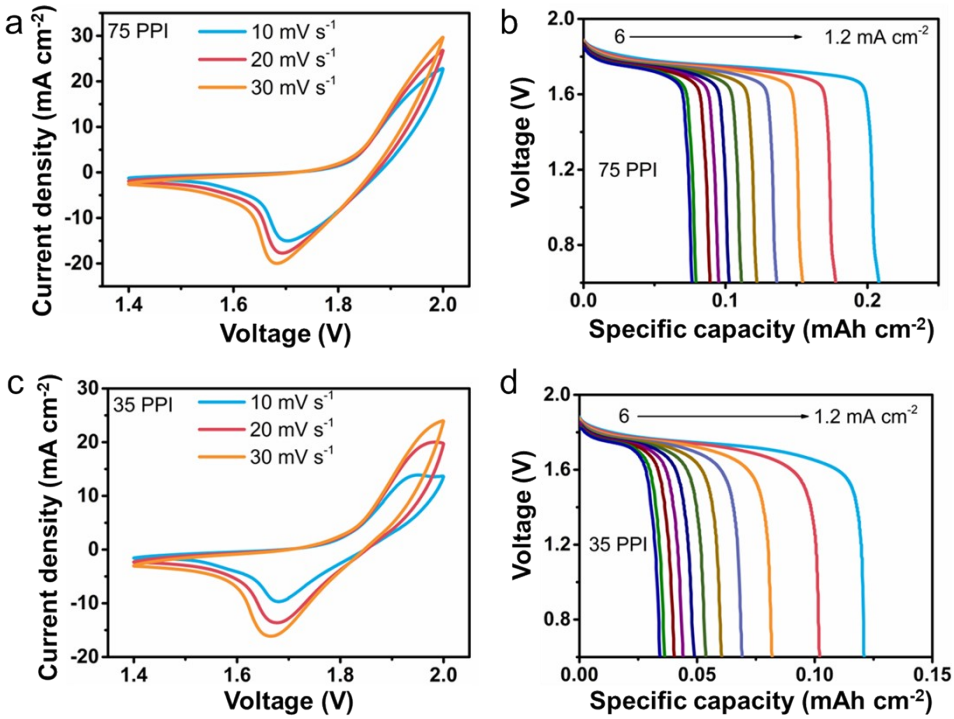


**Figure S13.** CV (a) and GCD curves (b) of E3DP-NZABs with 75 PPI pores size 3D structure. CV (c) and galvanostatic discharge curves (d) of E3DP-NZABs with 35 PPI pores sized 3D structure.

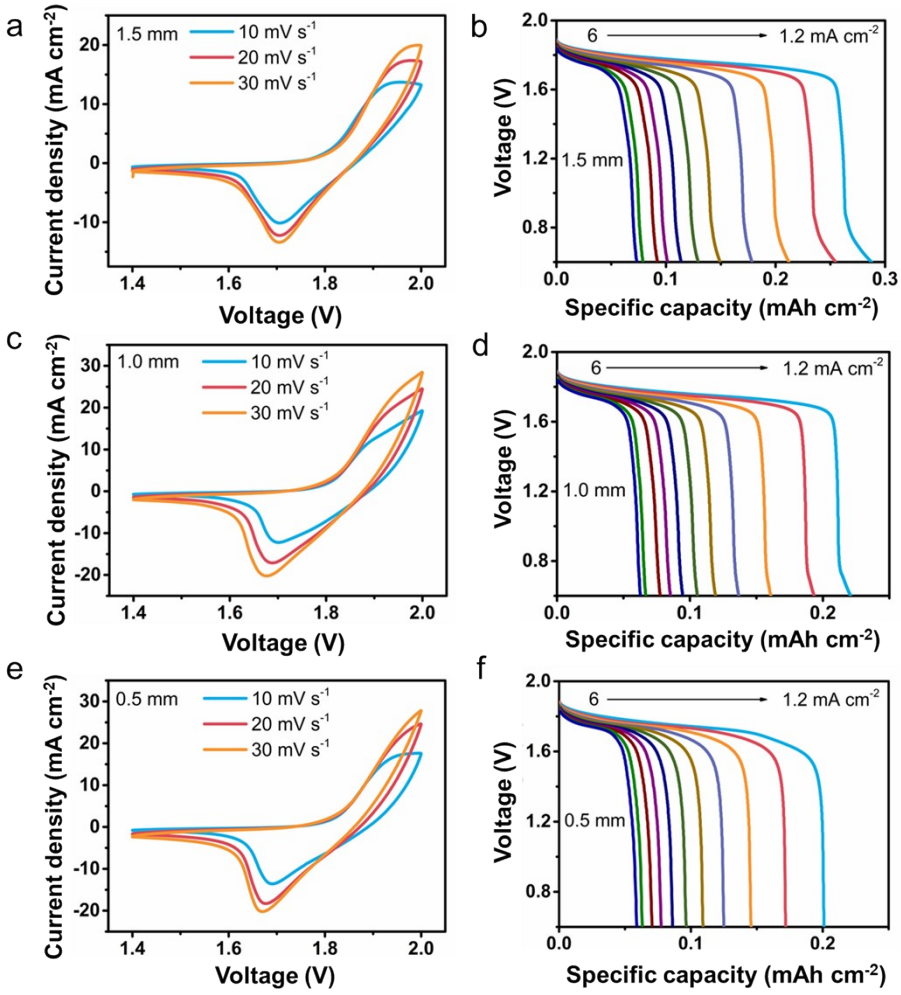


**Figure S14.** (a, b) CV (a) and galvanostatic discharge curves (b) of E3DP-NZABs with 1.5 mm thickness of 3D structure frames. (c,d) CV (c) and galvanostatic discharge curves (d) of E3DP-NZABs with 1.0 mm thickness 3D structure frames. (e,f) CV (e) and galvanostatic discharge curves (f) of E3DP-NZABs with 0.5 mm thickness of 3D structure frames.

## References

1. J. Yang, Z. Wang, Z. Wang, J. Zhang, Q. Zhang, P. P. Shum and L. Wei, *ACS Appl Mater Interfaces*, 2020, **12**, 12801-12808.

2. R. Wang, Y. Han, Z. Wang, J. Jiang, Y. Tong and X. Lu, *Advanced Functional Materials*, 2018, **28,** 1802157.